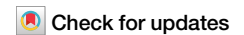




Limited influence of the Agulhas leakage on the Atlantic Meridional Overturning Circulation under present-day climate conditions



Ruize Zhang^{1,2}, Shantong Sun²✉, Zhaohui Chen^{1,2}✉ & Lixin Wu^{1,2}

The Agulhas leakage is expected to increase as the Southern Hemisphere westerly winds change under climate warming. An increased Agulhas leakage could potentially strengthen the Atlantic Meridional Overturning Circulation (AMOC). To date, however, it remains elusive how much this process could affect the AMOC, which is projected to weaken in the future. Here we carry out a suite of ocean-only simulations, which represent the present climate, and show that an arbitrary 10 Sv increase in the Agulhas leakage strengthens the AMOC by less than 1.3 Sv, which will unlikely substantially offset the projected AMOC weakening. The weak AMOC intensification arises due to compensation between subsurface warming and salinification. However, the AMOC responses to Agulhas leakage increases may depend on the climate background state. Initialized from a collapsed AMOC, which likely occurred during the glacial period, an increased Agulhas leakage can vigorously strengthen the AMOC due to a more unstable AMOC.

The Agulhas leakage, an inflow of warm, salty water from the Indian Ocean into the South Atlantic, is a crucial component of the global ocean overturning circulation^{1–3}. Due to the thermohaline differences between the Southeast Atlantic and Agulhas leakage water^{4,5} (Fig. 1a), variations in the Agulhas leakage can drive a net salt and heat exchange between ocean basins. This exchange can influence the thermohaline property in the North Atlantic^{6–8} and potentially modulate the Atlantic Meridional Overturning Circulation (AMOC) variability on interannual to millennial timescales^{9–11}. It has been suggested that an increase in the Agulhas leakage may trigger a recovery of the AMOC during the glacial period, supported by a correlation between the Agulhas leakage and AMOC transitions in paleoceanographic records^{12–15}.

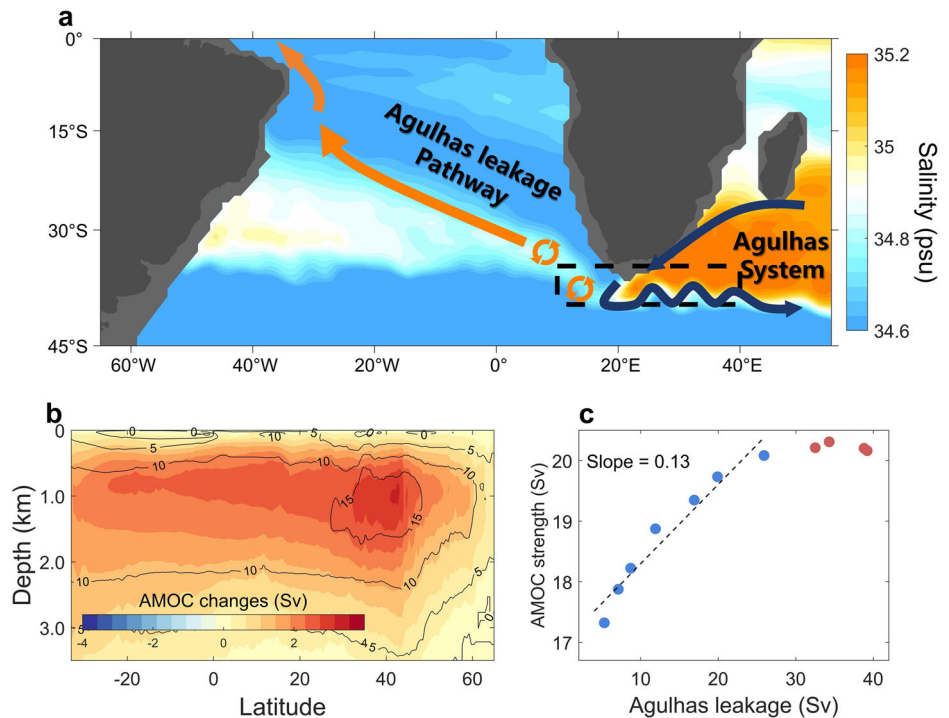
The Agulhas leakage is expected to increase^{16–20} as the Southern Hemisphere westerly winds change^{21–23} in the future warming climate. Among current state-of-the-art climate models, the multi-model ensemble-mean Agulhas leakage increases by 7.1 Sv, with a standard deviation of 4.7 Sv, over the 21st century under the high-emission scenario (Supplementary Fig. 1). The increased Agulhas leakage will bring more salty Indian Ocean water into the South Atlantic and may strengthen the AMOC. This process may partially offset the projected decline of the AMOC during the 21st century^{1,24–26} and affect the global climate^{27,28}. Previous studies that explore the

influence of changes in the Agulhas leakage on the AMOC typically apply a surface salinity/temperature perturbation in the southeast Atlantic Ocean in models^{11,12,29}. However, the thermohaline differences between the Southeast Atlantic and the Agulhas leakage water are most prominent at 500–1000 m depths, not at the sea surface^{30,31}. Thus, thermohaline perturbations applied at the sea surface cannot represent the vertical structure of thermohaline anomalies that may be induced by changes in the Agulhas leakage. As such, the AMOC response to surface perturbations may differ from that due to an increase in the Agulhas leakage. Thus, to date, it remains elusive how an increase in the Agulhas leakage may affect the AMOC in a warming climate.

In this study, we conduct a suite of idealized modelling experiments to identify the key physical processes by which the Agulhas leakage affect the AMOC. We show that an increase in the Agulhas leakage volume transport can indeed strengthen the AMOC, but the magnitude of the impact is limited in simulations that resemble the present climate. Based on a thermal wind framework for the AMOC, we attribute the limited AMOC responses to compensations between the subsurface warming and salinification effects as the Agulhas leakage increases. We also discuss the dependence on climate background states and find that an increase in Agulhas leakage may have played a more active role in AMOC changes during the glacial period.

¹Frontier Science Center for Deep Ocean Multisphere and Earth System (FDOMES)/Academy of Future Oceans and Physical Oceanography Laboratory, Ocean University of China, Qingdao, China. ²Laoshan Laboratory, Qingdao, China. ✉e-mail: stsun@qnlm.ac; chenzhaohui@ouc.edu.cn

Fig. 1 | AMOC changes in response to increases in the Agulhas leakage. **a** A schematic of the Agulhas leakage affecting the AMOC. The background color represents climatological mean salinity at 500 m depth from Argo observations. The black dashed box represents the region (10°E–40°E, 35°S–40°S) where we modify surface wind stress. The dark blue arrows represent the Agulhas Current system. The orange arrows represent the pathway of the Agulhas leakage water in the South Atlantic. **b** Changes in the AMOC streamfunction when the Agulhas leakage is increased from 5.3 Sv (“ref”) to 25.9 Sv. The black contours indicate the climatological AMOC streamfunction. **c** The AMOC strengths as the Agulhas leakage increases in our experiments. The AMOC in both (b) and (c) is evaluated at year 150 after modifying the Agulhas leakage in each experiment. The black dashed line in (c) represents a linear regression for Agulhas leakages below 30 Sv.



Limited AMOC strengthening by the Agulhas leakage

We use Parallel Ocean Program version 2 (POP2)³² (see “Experimental design” in Methods), the ocean component of the Community Earth System Model (CESM)³³ to carry out a series of ocean-only experiments. To isolate the impact of an increased Agulhas leakage on the AMOC^{11,12}, we modify the surface zonal wind stress in the Agulhas leakage region to the south of Africa (35°S–40°S, 10°E–40°E) (Fig. 1a and Supplementary Fig. 2)^{16,34}. This regional change in surface wind avoids direct modifications to the Southern Ocean upwelling, which returns North Atlantic deep water back to the sea surface^{35,36}. For the reference run (“Ref”), the Agulhas leakage is 5.3 Sv. This is weaker than the poorly constrained observational-based estimates of 15 Sv³⁷ and 21.3 ± 4.7 Sv³⁸. The AMOC strength in “Ref” is 17 Sv, close to observational-based estimates^{39–41}. Branched from “Ref”, we conduct a total of 10 perturbation experiments, in which we increase the Agulhas leakage to up to 40 Sv. In each perturbation experiment, the Agulhas leakage is roughly constant in time.

Our results show that an increase in the Agulhas leakage strengthens the AMOC (Fig. 1b), but it is unlikely able to offset the projected AMOC weakening in the 21st century. When the Agulhas leakage is lower than 30 Sv, a 10 Sv increase in the Agulhas leakage can only strengthen the AMOC by a maximum of 1.3 Sv, achieved after about 150 years, in our simulations (Fig. 1c). Considering the magnitude of Agulhas leakage changes projected by climate models (7.1 ± 4.7 Sv) (Supplementary Fig. 1), the AMOC changes due to Agulhas leakage increases are likely around 1 Sv, with a large uncertainty, under the high-emission scenario in 21st century. This is unlikely going to offset the projected AMOC decline -- the multi-model mean value of AMOC declines in CMIP models under the high-emission scenario is about 8 Sv⁴². When the Agulhas leakage is over 30 Sv, the AMOC strength levels off and does not respond to the Agulhas leakage increases (red points in Fig. 1c). This decoupling between the AMOC and the Agulhas leakage was also noted in a previous study based on a correlation analysis of a climate model⁴³. We will discuss the reason for the limited impacts of the Agulhas leakage on the AMOC in the following discussions.

Atlantic warming compensates for salinity increase

The limited impacts of Agulhas leakage increase on the AMOC are partly due to the compensating effects of warming and salinification in the Atlantic. To demonstrate this compensating effect, here we compare two

experiments, “AL17” and “AL26”, in which the Agulhas leakage is 16.9 Sv and 25.9 Sv, respectively. The Agulhas leakage in AL17 is close to the observation-based estimate^{37,38} and the Agulhas leakage increase from AL17 to AL26 is close to the multi-model ensemble-mean Agulhas leakage changes projected by CMIP models under the high-emission scenario. As the Agulhas leakage increases, more subtropical Indian Ocean water enters the Atlantic Ocean, increasing salinity and temperature throughout the upper 1500 m^{7,8}. The maximum thermohaline changes are found below the sea surface at 500–1000 m depths (Fig. 2a, b), consistent with the depths of Agulhas leakage water found in observations^{30,31}. In the subpolar North Atlantic, the temperature and salinity anomalies reach the deep ocean (3000–4000 m depth) through vertical mixing.

To quantify how thermohaline changes in the Atlantic Ocean due to increases in the Agulhas leakage affect the AMOC, we apply a thermal wind expression that relates the North Atlantic overturning to density differences between the deep-water formation region and the subtropical northern Atlantic^{44–46} (see “Thermal wind relation” in Methods; blue and green boxes in Fig. 2a). This relation follows directly from the thermal wind relationship if the meridional overturning transport were instead interpreted as a zonal overturning transport. A key assumption of this expression is that, in geostrophic balance, the meridional overturning transport and the zonal overturning transport are connected through continuity⁴⁴. The thermal wind relationship successfully reproduces the mean-state AMOC and its transient evolutions (Supplementary Fig. 3).

We decompose the AMOC changes into contributions due to thermal and haline changes using the thermal wind expression (see “Density changes decomposition” in Methods). Based on this decomposition, we find that the AMOC strengthening due to salinity increases is substantially compensated by the subsurface warming at high latitudes (Fig. 2). When the Agulhas leakage is less than 30 Sv, a 10 Sv increase in the Agulhas leakage would have strengthened the AMOC by 2.2 Sv, in absence of the temperature compensation (yellow line in Fig. 2c). The warming in high latitudes compensates for the AMOC strengthening by around 40% (orange line in Fig. 2c). This warming compensation was previously discussed¹¹, but its impact has been underestimated. This occurs because their temperature anomalies were located at the sea surface and quickly damped due to surface heat loss.

The Atlantic warming only partially compensates for the salinity increase because of the damping effect of surface heat loss in the subpolar

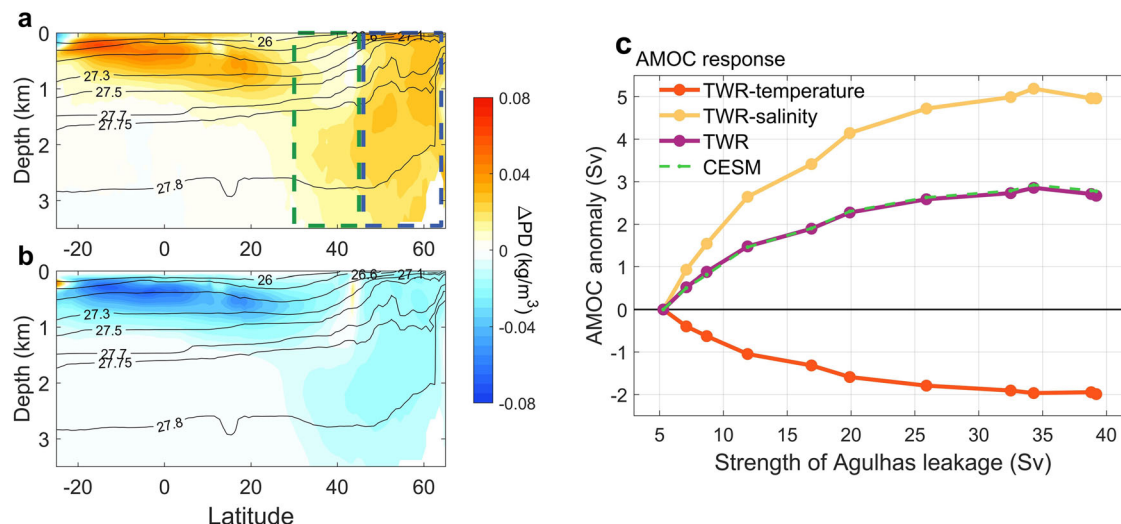


Fig. 2 | Compensating thermohaline changes in the Atlantic in response to increases in the Agulhas leakage. Zonal-mean potential density (referenced to sea surface) anomaly due to (a) salinity increase and (b) warming in the Atlantic Ocean. Black contours represent climatological zonal-mean potential density. The density anomaly is calculated as the difference between AL26 and AL 17, in which the Agulhas leakage is 25.9 Sv and 16.9 Sv, respectively, evaluated at year 150 after

modifying the Agulhas leakage. The blue and green dashed boxes in (a) represent the North Atlantic subpolar regions and southern interior Atlantic regions used in the thermal wind relation. c AMOC responses to Agulhas leakage increases, reconstructed from the thermal wind relationship (purple line) and its contributions due to temperature (orange) and salinity (yellow) changes. The AMOC strength reported by the model is plotted as a green dashed line for comparison.

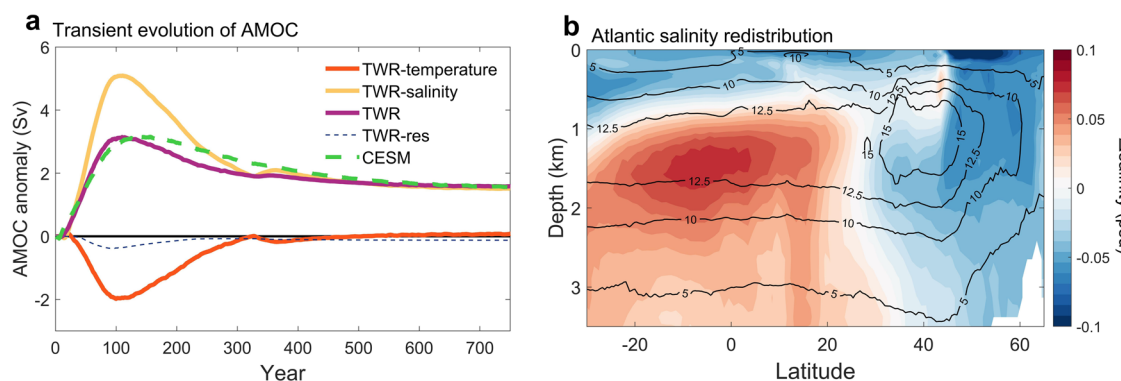


Fig. 3 | Salinity redistribution causing AMOC changes on multi-centennial timescales. a Transient AMOC responses as the Agulhas leakage is increased to 25.9 Sv (green dashed line). The AMOC is also reconstructed using the thermal wind relationship

(purple line) and decomposed into contributions due to temperature (orange line) and salinity (yellow line) changes. b Zonal mean salinity changes in the Atlantic Ocean from year 150 to year 1000. Black contours denote the climatological AMOC streamfunction.

North Atlantic and Southeast Atlantic. As isopycnals outcrop in the subpolar North Atlantic, subsurface warming spreads into the sea surface and enhances surface heat loss⁴⁷, which reduces subsurface warming in the subpolar North Atlantic (Supplementary Fig. 4). Similar processes occur in the Southeast Atlantic Ocean, the strengthened Agulhas leakage induces dramatic sea surface warming, which is quickly damped due to surface heat loss (Supplementary Fig. 5)^{11,17}. In coupled models, we expect this damping to be weaker, as the enhanced surface heat fluxes warm the atmosphere, which, in turn, decreases ocean heat loss⁴⁸. Thus, we argue that there will be an even weaker AMOC sensitivity to Agulhas leakage increases in the real ocean than our ocean-only model simulations.

Time-dependent AMOC responses to Agulhas leakage increases

The AMOC response to changes in the Agulhas leakage is also time dependent. Following an increase in the Agulhas leakage, the AMOC strengthening peaks around year 150 and then slowly declines over the next few centuries (green dashed line in Fig. 3a). This long-term decline of the AMOC after the initial strengthening is mainly due to changes in salinity (yellow and purple lines in Fig. 3a). Beyond the first 150 years, salinity keeps increasing in the deep ocean but decreases in the upper 1 km and the

subpolar North Atlantic (Fig. 3b). The long-term salinity increase in the deep ocean occurs as the initial salinity increase in the upper 1.5 km is mixed downward in the subpolar North Atlantic and spreads southward along the southward deep branch of the AMOC (Fig. 3b). On the other hand, the increased Agulhas leakage from the Indian Ocean would necessarily mean more water entering the Indian Ocean from the Pacific or the Southern Ocean to conserve volume, leading to a decrease in the Indian Ocean upper-ocean salinity (Supplementary Fig. 6)¹². This effect gradually decreases the efficiency of salty water export from the Indian Ocean and will cause surface freshening in the Atlantic Ocean beyond year 150.

These long-term adjustments are part of a global redistribution of salinity associated with increasing salinity in much of the global deep ocean (Supplementary Fig. 7). Taken together, our results suggest an even diminished influence of the Agulhas leakage on the AMOC on multi-centennial to millennial timescales (Supplementary Fig. 8).

Dependence on climate background states

The limited impact of Agulhas leakage increases on the AMOC appears to contradict paleoclimate records, which show correlations between the Agulhas leakage and AMOC transitions during the glacial-interglacial cycles^{1,12-15}. For example, the onset of increased Agulhas leakage was often

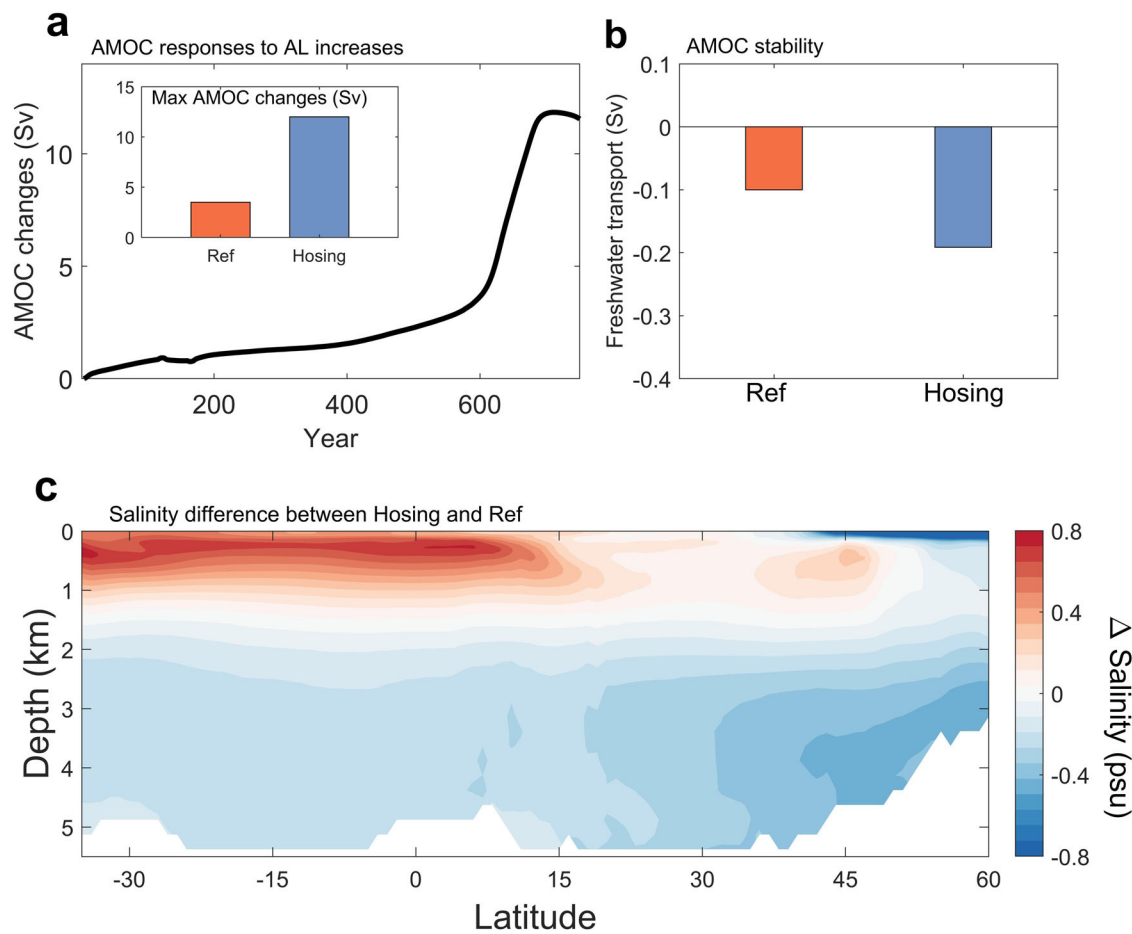


Fig. 4 | Dependence of the AMOC responses to Agulhas leakage increase on climate background. **a** AMOC responses after the Agulhas leakage is increased to 26 Sv, initialized from the hosing experiment (black line; Hos26). The inset compares the maximum AMOC strengthening after increasing the Agulhas leakage between two experiments with different initial conditions (ref vs Hosing). The

AMOC changes are evaluated as anomalies from Hosing, which runs in parallel with Hos26. **b** The freshwater transport across the southern boundary of Atlantic Ocean by overturning circulation F_{ov} in Ref (orange bar) and Hosing (blue bar) (see “AMOC stability” in Methods). **c** Zonal-mean salinity differences between Hosing and Ref (Hosing-Ref) in the Atlantic Ocean.

found to take place during late glacial conditions when the glacial ice volume was maximal, suggesting a potential role of the Agulhas leakage in glacial termination and the recovery of AMOC¹³.

The paleoclimate record was supported by a modelling study, in which an increase in the salinity of the Agulhas leakage leads to an increase in the AMOC strength from a collapsed state by more than 10 Sv¹². The 10 Sv increase in the AMOC strength cannot be explained by the absence of warming compensations. Instead, this contradiction may be reconciled by considering the dependence on climate background states. The initial AMOC state can affect the salinity distribution in the South Atlantic and thereby, influence the AMOC stability^{49,50}. To demonstrate this idea, we create an additional set of experiments, including a hosing experiment (“Hosing”) in which the AMOC strength is weakened from 17 Sv to around 5 Sv by applying a freshwater perturbation in the subpolar North Atlantic (see “Experimental design” in Methods). Starting from the AMOC-collapse state, we increase the Agulhas leakage from 5.3 Sv to 26 Sv (“Hos26”). After about 600 years, the AMOC fully recovers and strengthens by over 12 Sv (Fig. 4a). The 600-year time scale is much longer than the 150-year response time scale with an active AMOC discussed above. This is because a weaker AMOC is less efficient in transporting salinity anomalies from the South Atlantic into the subpolar North Atlantic, where deep water forms.

The larger AMOC responses to Agulhas leakage increases can be explained by the differing stability level of the AMOC^{50–52}, which is quantified using the freshwater transport by the overturning circulation across the southern boundary of the Atlantic Ocean, F_{ov} (see “AMOC stability” in

Methods). For a negative F_{ov} , it means the AMOC exports freshwater out of the Atlantic Ocean and thus, a small increase in the AMOC increases salinity in the Atlantic and leads to an even stronger AMOC, i.e., a positive feedback. For a positive F_{ov} , the opposite is happening and a negative feedback leads to a more stable AMOC. Indeed, the collapsed AMOC increases salinity in the upper South Atlantic²⁵ (Fig. 4c), leading to a more negative F_{ov} (Fig. 4b), i.e., the AMOC may have become more unstable when it is in a collapsed state. Thus, during the glacial period when the AMOC was collapsed, the AMOC may become more unstable and an increase in the Agulhas leakage could have played an important role in resuming the AMOC.

Discussion

The Agulhas leakage is expected to increase in a warming climate as the Southern Hemisphere westerly wind shifts poleward and strengthens, potentially strengthening the AMOC during the 21st century. We examined the AMOC responses to increases in the Agulhas leakage using a series of modelling experiments. We show that an increase in the Agulhas leakage can indeed strengthen the AMOC, but the strengthening is far from offsetting the AMOC decline projected for the 21st century in a warming climate. The limited impacts of the Agulhas leakage on the AMOC are partly due to a cancellation between subsurface warming and salinification in the Atlantic. On longer terms, the impacts of Agulhas leakage are even diminished due to a global redistribution of salinity. Nevertheless, the Agulhas leakage may have played a critical role in the AMOC transitions during the glacial period. When the AMOC is collapsed, the AMOC is more

unstable and an increase in the Agulhas leakage may trigger the recovery of the AMOC, amplified by the basin-scale salt-advection feedback in the Atlantic Ocean.

Our ocean models cannot resolve meso-scale eddies, including the Agulhas rings. Thus, the water exchange between the Indian Ocean and the South Atlantic is in the form of mean flows. The thermohaline properties reaching the North Atlantic may be diluted in our model experiments, leading to underestimated thermohaline responses⁴³. However, we reckon that the processes discussed in this study are still relevant for the real ocean. In the future, high-resolution modelling experiments are still needed to address this caveat.

Current state-of-the-art climate models typically overestimate the Agulhas leakage due to their coarse resolutions. For example, the multi-model ensemble-mean Agulhas leakage is about 30 Sv in CMIP6 (Supplementary Fig. 1)⁵³, almost two times as large as in observations^{37,38}. The excessive Agulhas leakage reduces thermohaline contrast between the Southeast Atlantic and the Indian Ocean (Supplementary Fig. 9 and Supplementary Fig. 10) and may contribute to the salinity bias in the Atlantic Ocean⁵⁴. The large Agulhas leakage also suggests a further reduced sensitivity of the AMOC to future Agulhas leakage increases in climate models (red points in Fig. 1b)⁴⁵, consistent with the lack of inter-model correlations between the AMOC and Agulhas leakage in CMIP6 (Supplementary Fig. 11). Due to the overestimated Agulhas leakage in CMIP models, the AMOC responses to Agulhas leakage increases may also be underestimated⁴³ and hence, lead to a slight overestimation of future AMOC declines in response to anthropogenic warming.

Methods

Experimental design

In this study, we conduct a series of ocean-only sensitivity experiments based on the Parallel Ocean Program version 2 (POP2)³², which is the ocean component of the Community Earth System Model (CESM)³³. The model has a nominal 1° resolution in the horizontal and 60 layers in the vertical, ranging from 10 m at the top to 250 m at the bottom. The model is initialized from a state of rest with observed January-mean climatological Polar Science Center Hydrographic Climatology (PHC2) potential temperature and salinity. The model is forced with normal year forcing from the Coordinated Ocean-Ice Reference Experiments version2 (COREv2) dataset⁵⁵, including air temperature, specific humidity, long-wave radiation, precipitation, runoff, shortwave radiation, and wind speed. In the simulation, surface salinity is weakly restored to observed climatological sea surface salinity with a restoring timescale of 4 years³². Unresolved mesoscale eddies are parameterized using the Gent-McWilliams scheme with a thickness diffusivity that is a function of local density stratification. Vertical mixing is handled by the non-local K-Profile Parameterization (KPP) scheme. We spin up model for 600 years (“ref”). Another ten sensitivity experiments were branched from year 601 and integrated for another 1000 years.

To investigate the impact of Agulhas leakage increases on the AMOC^{11,12}, we modify the surface zonal wind stress in the Agulhas leakage region to the south of Africa (35°S–40°S, 10°E–40°E) (Fig. 1a and Supplementary Fig. 2)^{16,34}. This regional change in surface wind is confined to the Agulhas leakage region to avoid direct modifications to the Southern Ocean upwelling, which returns North Atlantic Deep Water back to the sea surface^{35,36}. For the reference run (“Ref”), the Agulhas leakage is 5.3 Sv, which is weaker than the observation-based estimate^{37,38}. In Ref, the AMOC strength is 17 Sv, close to observation-based estimates^{39–41}. The volume transport of Antarctic Circumpolar Current (ACC) across the Drake Passage is 119 Sv, slightly smaller than the observation^{56,57}. Because the model is forced with repeating normal year external forcing, the inter-annual variability of the ocean circulation is weak. The inter-annual variability of the Agulhas Current and the AMOC is less than 0.5 Sv. Branched from “Ref”, we modify local surface zonal wind stress and conduct a total of 10 perturbation experiments (see Supplementary Note 1 and Supplementary Table 1), in which we increase the Agulhas leakage to up to 40 Sv. The

thermohaline evaluation of the experiments is provided in the Supplementary Information (see Supplementary Note 2 and Supplementary Fig. 12).

To investigate the impact of Agulhas leakage increases on the AMOC recovery from a collapsed state, we conduct another suite of experiments, initialized from a “hosing” experiment in which the AMOC collapses. The “hosing” experiment (“Hosing”) was designed to represent a collapsed AMOC state. This is achieved by applying a freshwater perturbation of 0.06 Sv in the subpolar North Atlantic (50–60°N, 60°W–0°), initialized from Ref at year 600. Branched from Hosing at Year 200, when the AMOC has collapsed, we conduct another experiment that runs in parallel with Hosing but with increased Agulhas leakage to 26 Sv (“Hos26”).

Agulhas leakage estimate

In the modelling experiment, the Agulhas leakage is estimated using a Lagrangian method based on “Probably A Really Computationally Efficient Lagrangian Simulator” (Parcels)^{58,59}. We use 10-day mean 3-dimension velocity during model years 751–755 in each experiment to estimate the Lagrangian pathway of Agulhas leakage water, which is integrated using the fourth-order Runge-Kutta method with a time step of 1 hour. The velocity fields are linearly interpolated in space and time. We release particles every ten days at the section of the Agulhas Current Time-series Experiment (blue line in Supplementary Fig. 13a) with a longitudinal spacing of 0.1° over the upper 1500 m. The particles are released throughout model year 751 in each experiment and tracked for four years. In total, we released 20,592 particles in each experiment and each of the particles represents a fraction of the Agulhas Current volume transport (Supplementary Fig. 13b). The location of each particle is saved every ten days. Those particles that cross the Good Hope section (red line in Supplementary Fig. 13a) at least once are counted as Agulhas leakage. As an example, in AL17, a total of 3680 particles crossed the Good Hope section, representing a volume transport by Agulhas leakage of 16.9 Sv. We also test the sensitivity of our results to the number of particles. When we release the particles every 5 days, the estimated strength of Agulhas leakage slightly changes, but within 1.5 Sv. Here we also use a Eulerian method to estimate the Agulhas leakage, defined as the volume transport across the section between (11.5°E, 38.5°S) and (18.5°E, 31.5°S) (green line in Supplementary Fig. 2b) over the upper 1500 m. The Eulerian estimate largely reproduces the Lagrangian estimate of Agulhas leakage with a standard error of 2.1 Sv (Supplementary Fig. 13). The correlation between these two estimates is at 0.98.

Thermal wind relation

To explore the mechanism in causing the AMOC changes, we use a thermal wind expression^{44–46}, in which the strengthen of AMOC in the North Atlantic isopycnal-outcropping region is dynamically linked to the density difference between the deep-water formation region and the subtropical northern Atlantic.

$$\frac{\partial^2 \psi}{\partial z^2} = -\frac{g}{\rho_0 f} (\rho_n - \rho_s) \quad (1)$$

where ψ is the meridional overturning circulation streamfunction, g is the gravity acceleration ($g = 9.8 \text{ m s}^{-2}$), ρ_0 is the reference density of sea water ($\rho_0 = 1020 \text{ kg m}^{-3}$), f is the Coriolis parameter around 45°N ($f = 1.05 \times 10^{-4} \text{ s}^{-1}$), ρ_n is the potential density in the North Atlantic isopycnal-outcropping region (averaged from 45°N to 65°N), ρ_s is potential density in the Southern interior Atlantic Ocean (averaged from 30°N to 45°N). To solve for (1), we use $\psi = 0$ at the surface and bottom of the ocean as boundary conditions. In this formulation, the meridional volume transport is related, by volume conservation, to the zonal volume transport, which can be reconstructed from the meridional density gradient in the North Atlantic. Here, we choose the regions north of 45°N to represent the deep-water formation region and the region south of 45°N to represent the interior basin. Similar approaches have been used in previous studies to reconstruct AMOC changes from temperature and salinity fields⁴⁶.

Density changes decomposition

To isolate the effects of temperature and salinity changes on the AMOC, we decompose the density changes into temperature-induced and salinity-induced contributions:

$$\begin{aligned}\Delta\rho &= \rho(T_2, S_2, p) - \rho(T_1, S_1, p) \\ &= \rho(T_2, S_1, p) - \rho(T_1, S_1, p) + \rho(T_1, S_2, p) - \rho(T_1, S_1, p) + Res \\ &= \Delta\rho_T + \Delta\rho_S + Res\end{aligned}\quad (2)$$

where $\rho(T, S, p)$ is the state equation of sea water, using the UNESCO 1983 (EOS 80) polynomial⁶⁰, Res is the residual due to nonlinearity in the equation of state.

AMOC stability

The stability of AMOC is assessed by calculating the meridional freshwater transport across the southern boundary of the Atlantic Ocean by the overturning circulation^{44,45}:

$$F_{ov} = -\frac{1}{S_0} \int_{x^e}^{x^w} \int_{-H}^0 (v(x, z) - v_m) \langle S(x, z) \rangle dz dx \quad (3)$$

where v is northward velocity and S is salinity, $\langle \rangle$ denotes zonal mean across the Atlantic Ocean, $S_0 = 35$ psu, v_m denotes the mean velocity across the whole Atlantic zonal section, x^w and x^e is the west and east boundary of the Atlantic Ocean, H is the depth of the ocean. The freshwater transport is estimated at 32°S, the southern boundary of Atlantic Ocean. If the AMOC exports freshwater, $F_{ov} < 0$, a small increase of the AMOC strength will be amplified by exporting more freshwater, i.e., a positive salt-advection feedback^{46,47}. Therefore, a more negative F_{ov} tends to suggest a more unstable AMOC. Conversely, if the freshwater transport F_{ov} is positive, the AMOC is more stable and the system may be in a monostable regime⁴⁷. Because the atmospheric forcing in the ocean-only experiment is based on observations, the salinity bias at the southern boundary of the Atlantic Ocean is smaller (See Supplementary Note 2 and Supplementary Fig. 14). The smaller salinity biases lead to a negative freshwater transport by the overturning circulation, F_{ov} , across the southern boundary of Atlantic Ocean in our experiment that is more consistent with observations^{61,62}.

Climate model simulations

To evaluate how is the Agulhas leakage simulated in current state-of-the-art climate models, we examined 40 climate models, participating in the Coupled Model Intercomparison Project Phase 6 (CMIP6), including ACCESS-CM2, ACCESS-ESM1-5, AWI-CM-1-1-MR, AWI-ESM-1-1-LR, BCC-CSM2-MR, BCC-ESM1, CAS-ESM2-0, CESM2-FV2, CESM2-WACCM, CESM2, CMCC-CM2-SR5, CMCC-ESM2, CNRM-CM6-1, CNRM-ESM2-1, CanESM5-CanOE, CanESM5, E3SM-1-1, EC-Earth3-AerChem, EC-Earth3-CC, EC-Earth3-Veg, EC-Earth3, FIO-ESM-2-0, GFDL-CM4, GISS-E2-1-G-CC, GISS-E2-1-G, HadGEM3-GC31-LL, HadGEM3-GC31-HM, HadGEM3-GC31-MM, INM-CM4-8, INM-CM5-0, IPSL-CM5A2-INCA, KIOST-ESM, MCM-UA-1-0, MIROC6, NorESM2-LM, NorESM2-MM, SAM0-UNICON, TaiESM1, UKESM1-0-LL, UKESM1-1-LL. We use results from simulations conducted under the historical scenario to assess the relationship between the Agulhas leakage and AMOC. Historical scenario simulations in the CMIP6 are conducted under the historical observed external forcing, including greenhouse-gas concentration, ozone, aerosols, and natural variability over the years from 1850–2014. All model outputs are interpolated to the same 1° latitude by 1° longitude grid before analysis. To compare with observations, the CMIP6 climatology salinity and temperature data are averaged from 2000 to 2014 in the historical simulation.

For the Agulhas leakage changes projected for the 21st century, we use the multi-model ensemble mean of the Agulhas leakage under high-emission scenario (“SSP585”) from 2015 to 2100. These low-resolution climate models cannot resolve mesoscale processes, which are often

parameterized, and thus, may introduce biases. To account for this, we estimate the Agulhas leakage changes in high-resolution climate model from HighresMIP (CESM-H, CMCC-CM2-HR4, CMCC-CM2-VHR4, CNRM-CM6-1-HR, EC-Earth3P-HR, HadGEM3-GC31-HH, HadGEM3-GC31-HM, HadGEM3-GC31-MM, CESM2-WACCM)^{63,64}, in which the ocean component has a horizontal resolution of about 0.1° (eddy-resolving) or 0.25° (eddy-permitting) in the mid-latitudes.

Observation data

In this study, we also use the Roemmich-Gilson Argo Climatology dataset⁶⁵ for comparison. The Argo Program has 20 years of global coverage, with 12,000 data profiles each month, and provide a baseline for evaluating the thermohaline property in the upper 2000 m. The dataset is derived from Argo float observation data and averaged from January 2004 to December 2018, covering 64.5°S to 79.5°N on 1° resolution.

Data availability

The CMIP6 outputs are available from the ESGF portals (<https://esgf-node.llnl.gov/projects/cmip6/>). The Roemmich-Gilson Argo observation thermohaline Climatology dataset is available from https://sio-argo.ucsd.edu/RG_Climatology.html. The ocean-only model data is generated by the POP2 model, and its external forcing COREv2 is available from input-data repository of CESM (<https://svn-ccsm-inputdata.cgd.ucar.edu/trunk/>).

Code availability

Codes for the main results are available in figshare (https://figshare.com/articles/dataset/AL_AMOCdata_code_zip/25118093). The CESM is freely available as open-source code from <http://www.cesm.ucar.edu/models/cesm1.1>.

Received: 27 February 2024; Accepted: 4 February 2025;

Published online: 21 February 2025

References

1. Beal, L. M. et al. On the role of the Agulhas system in ocean circulation and climate. *Nature* **472**, 429–436 (2011).
2. Cessi, P. & Jones, C. S. Warm-Route versus Cold-Route Interbasin Exchange in the Meridional Overturning Circulation. *J. Phys. Oceanogr.* **47**, 1981–1997 (2017).
3. R hs, S. et al. Robust estimates for the decadal evolution of Agulhas leakage from the 1960s to the 2010s. *Commun. Earth Environ.* **3**, 318 (2022).
4. Gordon, A. L. Inter-ocean exchange of thermocline water. *J. Geophys. Res. Oceans* **91**, 5037–5046 (1986).
5. de Ruijter, W. P. M. et al. Indian-Atlantic inter-ocean exchange: Dynamics, estimation and impact. *J. Geophys. Res. Oceans* **104**, 20885–20910 (1999).
6. R hs, S., Durgadoo, J. V., Behrens, E. & Biastoch, A. Advective timescales and pathways of Agulhas leakage. *Geophys. Res. Lett.* **40**, 3997–4000 (2013).
7. Biastoch, A. et al. Atlantic multi-decadal oscillation covaries with Agulhas leakage. *Nat. Commun.* **6**, 10082 (2015).
8. L bbecke, J. F., Durgadoo, J. V. & Biastoch, A. Contribution of increased Agulhas leakage to Tropical Atlantic Warming. *J. Clim.* **28**, 9697–9706 (2015).
9. Biastoch, A., B ning, C. W. & Lutjeharms, J. R. E. Agulhas leakage dynamics affects decadal variability in Atlantic overturning circulation. *Nature* **456**, 489–492 (2008).
10. Weaver, A. J. et al. Stability of the Atlantic meridional overturning circulation: A model intercomparison. *Geophys. Res. Lett.* **39**, L20709 (2012).
11. Weijer, W., De Ruijter, W. P. M., Sterl, A. & Drijfhout, S. S. Response of the Atlantic overturning circulation to South Atlantic sources of buoyancy. *Global Planet. Change* **34**, 293–311 (2002).

12. Nuber, S. et al. Indian Ocean salinity build-up primes deglacial ocean circulation recovery. *Nature* **617**, 306–311 (2023).
13. Peeters, F. J. C. et al. Vigorous exchange between the Indian and Atlantic oceans at the end of the past five glacial periods. *Nature* **430**, 661–665 (2004).
14. Caley, T., Giraudeau, J., Malaizé, B., Rossignol, L. & Pierre, C. Agulhas leakage as a key process in the modes of Quaternary climate changes. *Proc. Natl. Acad. Sci.* **109**, 6835–6839 (2012).
15. Knorr, G. & Lohmann, G. Southern Ocean origin for the resumption of Atlantic thermohaline circulation during deglaciation. *Nature* **424**, 532–536 (2003).
16. Durgadoo, J. V., Loveday, B. R., Reason, C. J. C., Penven, P. & Biastoch, A. Agulhas leakage Predominantly Responds to the Southern Hemisphere Westerlies. *J. Phys. Oceanogr.* **43**, 2113–2131 (2013).
17. Biastoch, A. & Böning, C. W. Anthropogenic impact on Agulhas leakage. *Geophys. Res. Lett.* **40**, 1138–1143 (2013).
18. Biastoch, A., Böning, C. W., Schwarzkopf, F. U. & Lutjeharms, J. R. E. Increase in Agulhas leakage due to poleward shift of Southern Hemisphere westerlies. *Nature* **462**, 495–498 (2009).
19. Rouault, M., Penven, P. & Pohl, B. Warming in the Agulhas Current system since the 1980's. *Geophys. Res. Lett.* **36**, L12602 (2009).
20. Marcello, F., Tonelli, M., Ferrero, B. & Wainer, I. Projected Atlantic overturning slow-down is to be compensated by a strengthened South Atlantic subtropical gyre. *Commun. Earth Environ.* **4**, 92 (2023).
21. Cai, W. Antarctic ozone depletion causes an intensification of the Southern Ocean super-gyre circulation. *Geophys. Res. Lett.* **33**, L03712 (2006).
22. Goyal, R., Sen Gupta, A., Jucker, M. & England, M. H. Historical and Projected Changes in the Southern Hemisphere Surface Westerlies. *Geophys. Res. Lett.* **48**, e2020GL090849 (2021).
23. Sen Gupta, A. et al. Projected Changes to the Southern Hemisphere Ocean and Sea Ice in the IPCC AR4 Climate Models. *J. Clim.* **22**, 3047–3078 (2009).
24. Rahmstorf, S. et al. Exceptional twentieth-century slowdown in Atlantic Ocean overturning circulation. *Nat. Clim. Change* **5**, 475–480 (2015).
25. Zhu, C. & Liu, Z. Weakening Atlantic overturning circulation causes South Atlantic salinity pile-up. *Nat. Clim. Change* **10**, 998–1003 (2020).
26. Bellomo, K., Angeloni, M., Corti, S. & von Hardenberg, J. Future climate change shaped by inter-model differences in Atlantic meridional overturning circulation response. *Nat. Commun.* **12**, 3659 (2021).
27. Liu, W., Fedorov, A. V., Xie, S.-P. & Hu, S. Climate impacts of a weakened Atlantic Meridional Overturning Circulation in a warming climate. *Sci. Adv.* **6**, eaaz4876 (2020).
28. Zhang, R. et al. A Review of the Role of the Atlantic Meridional Overturning Circulation in Atlantic Multidecadal Variability and Associated Climate Impacts. *Rev. Geophys.* **57**, 316–375 (2019).
29. Cimadoribus, A. A., Drijfhout, S. S., den Toom, M. & Dijkstra, H. A. Sensitivity of the Atlantic meridional overturning circulation to South Atlantic freshwater anomalies. *Clim. Dyn.* **39**, 2291–2306 (2012).
30. Guerra, L. A. A., Paiva, A. M. & Chassignet, E. P. On the translation of Agulhas rings to the western South Atlantic Ocean. *Deep Sea Res. Part Oceanogr. Res. Pap.* **139**, 104–113 (2018).
31. Laxenaire, R., Speich, S. & Stegner, A. Evolution of the thermohaline structure of one Agulhas ring reconstructed from satellite altimetry and argo floats. *J. Geophys. Res. Oceans* **124**, 8969–9003 (2019).
32. Danabasoglu, G. et al. The CCSM4 ocean component. *J. Clim.* **25**, 1361–1389 (2012).
33. Gent, P. R. et al. The community climate system model version 4. *J. Clim.* **24**, 4973–4991 (2011).
34. Bard, E. & Rickaby, R. E. M. Migration of the subtropical front as a modulator of glacial climate. *Nature* **460**, 380–383 (2009).
35. Johnson, H. L., Cessi, P., Marshall, D. P., Schloesser, F. & Spall, M. A. Recent contributions of theory to our understanding of the Atlantic meridional overturning circulation. *J. Geophys. Res. Oceans* **124**, 5376–5399 (2019).
36. Marshall, J. & Speer, K. Closure of the meridional overturning circulation through Southern Ocean upwelling. *Nat. Geosci.* **5**, 171–180 (2012).
37. Richardson, P. L. Agulhas leakage into the Atlantic estimated with subsurface floats and surface drifters. *Deep Sea Res. Part Oceanogr. Res. Pap.* **54**, 1361–1389 (2007).
38. Daher, H., Beal, L. M. & Schwarzkopf, F. U. A new improved estimation of Agulhas leakage using observations and simulations of lagrangian floats and drifters. *J. Geophys. Res. Oceans* **125**, e2019JC015753 (2020).
39. Cunningham, S. A. et al. Temporal variability of the Atlantic meridional overturning circulation at 26.5°N. *Science* **317**, 935–938 (2007).
40. Rousselet, L., Cessi, P. & Forget, G. Coupling of the mid-depth and abyssal components of the global overturning circulation according to a state estimate. *Sci. Adv.* **7**, eabf5478 (2021).
41. Cessi, P. The Global Overturning Circulation. *Annual Review of Marine Science* **11**, 249–270 (2019).
42. Weijer, W., Cheng, W., Garuba, O. A., Hu, A. & Nadiga, B. T. CMIP6 models predict significant 21st century decline of the atlantic meridional overturning circulation. *Geophys. Res. Lett.* **47**, e2019GL086075 (2020).
43. Weijer, W. & van Sebille, E. Impact of Agulhas leakage on the Atlantic overturning circulation in the CCSM4. *J. Clim.* **27**, 101–110 (2014).
44. Jansen, M. F., Nadeau, L.-P. & Merlis, T. M. Transient versus equilibrium response of the ocean's overturning circulation to warming. *J. Clim.* **31**, 5147–5163 (2018).
45. Nikurashin, M. & Vallis, G. A theory of the interhemispheric meridional overturning circulation and associated stratification. *J. Phys. Oceanogr.* **42**, 1652–1667 (2012).
46. Bonan, D. B., Thompson, A. F., Newsom, E. R., Sun, S. & Rugenstein, M. Transient and equilibrium responses of the atlantic overturning circulation to warming in coupled climate models: the role of temperature and salinity. *J. Clim.* **35**, 5173–5193 (2022).
47. Banks, H. T., Stark, S. & Keen, A. B. The adjustment of the coupled climate model HadGEM1 toward equilibrium and the impact on global climate. *J. Clim.* **20**, 5815–5826 (2007).
48. Souza, J. M. A. C., Chapron, B. & Autret, E. The surface thermal signature and air–sea coupling over the Agulhas rings propagating in the South Atlantic Ocean interior. *Ocean Sci.* **10**, 633–644 (2014).
49. Stommel, H. Thermohaline convection with two stable regimes of flow. *Tellus* **13**, 224–230 (1961).
50. Liu, W., Liu, Z. & Hu, A. The stability of an evolving Atlantic meridional overturning circulation. *Geophys. Res. Lett.* **40**, 1562–1568 (2013).
51. Weijer, W. et al. Stability of the Atlantic meridional overturning circulation: a review and synthesis. *J. Geophys. Res. Oceans* **124**, 5336–5375 (2019).
52. Gent, P. R. A commentary on the Atlantic meridional overturning circulation stability in climate models. *Ocean Model.* **122**, 57–66 (2018).
53. Eyring, V. et al. Overview of the coupled model intercomparison project phase 6 (CMIP6) experimental design and organization. *Geosci. Model Dev.* **9**, 1937–1958 (2016).
54. Intergovernmental Panel on Climate Change (IPCC). *Climate Change 2021 – The Physical Science Basis: Working Group I Contribution to the Sixth Assessment Report of the Intergovernmental Panel on Climate Change*. (Cambridge University Press, 2023). <https://doi.org/10.1017/9781009157896>.
55. Griffies, S. M. et al. Coordinated ocean-ice reference experiments (COREs). *Ocean Model.* **26**, 1–46 (2009).
56. Donohue, K. A., Tracey, K. L., Watts, D. R., Chidichimo, M. P. & Chereskin, T. K. Mean Antarctic circumpolar current transport measured in drake passage. *Geophys. Res. Lett.* **43**, 11760–11767 (2016).

57. Whitworth, T. & Peterson, R. G. Volume transport of the antarctic circumpolar current from bottom pressure measurements. *J. Phys. Oceanogr.* **15**, 810–816 (1985).
58. Schmidt, C., Schwarzkopf, F. U., Rühls, S. & Biastoch, A. Characteristics and robustness of Agulhas leakage estimates: an inter-comparison study of Lagrangian methods. *Ocean Sci.* **17**, 1067–1080 (2021).
59. Delandmeter, P. & van Sebille, E. The Parcels v2.0 Lagrangian framework: new field interpolation schemes. *Geosci. Model Dev.* **12**, 3571–3584 (2019).
60. Fofonoff, P. & Millard, R. C. Algorithms for computation of fundamental properties of seawater. *UNESCO Techn. Papers in Mar. Sci.* **44** (UNESCO, 1983).
61. Arumi-Planas, C. et al. A multi-data set analysis of the freshwater transport by the Atlantic meridional overturning circulation at nominally 34.5 °S. *J. Geophys. Res. Oceans* **129**, e2023JC020558 (2024).
62. Rahmstorf, S. On the freshwater forcing and transport of the Atlantic thermohaline circulation. *Clim. Dyn.* **12**, 799–811 (1996).
63. Chang, P. et al. An unprecedented set of high-resolution earth system simulations for understanding multiscale interactions in climate variability and change. *J. Adv. Model. Earth Syst.* **12**, e2020MS002298 (2020).
64. Haarsma, R. J. et al. High resolution model intercomparison project (HighResMIP v1.0) for CMIP6. *Geosci. Model Dev.* **9**, 4185–4208 (2016).
65. Roemmich, D. & Gilson, J. The 2004–2008 mean and annual cycle of temperature, salinity, and steric height in the global ocean from the Argo Program. *Prog. Oceanogr.* **82**, 81–100 (2009).

Acknowledgements

This research is supported by the National Natural Science Foundation of China (42225601 and 42076009). Z. Chen is partly supported by the Supporting Funds for Leading Talents (2022GJJLJRC02-014). We thank Yan Wang for a helpful discussion.

Author contributions

S.S. and Z.C. conceived the study. R.Z. carried out the model experiments and did the analyses. R.Z. and S.S. wrote the manuscript. Z.C. and L.W. contribute to discussions and revising the manuscript.

Competing interests

The authors declare no competing interests.

Additional information

Supplementary information The online version contains supplementary material available at <https://doi.org/10.1038/s43247-025-02097-4>.

Correspondence and requests for materials should be addressed to Shantong Sun or Zhaohui Chen.

Peer review information *Communications Earth & Environment* thanks Louise Rousselet, Christina Schmidt and the other, anonymous, reviewer(s) for their contribution to the peer review of this work. Primary Handling Editors: Viviane Menezes, Heike Langenberg. A peer review file is available.

Reprints and permissions information is available at <http://www.nature.com/reprints>

Publisher's note Springer Nature remains neutral with regard to jurisdictional claims in published maps and institutional affiliations.

Open Access This article is licensed under a Creative Commons Attribution-NonCommercial-NoDerivatives 4.0 International License, which permits any non-commercial use, sharing, distribution and reproduction in any medium or format, as long as you give appropriate credit to the original author(s) and the source, provide a link to the Creative Commons licence, and indicate if you modified the licensed material. You do not have permission under this licence to share adapted material derived from this article or parts of it. The images or other third party material in this article are included in the article's Creative Commons licence, unless indicated otherwise in a credit line to the material. If material is not included in the article's Creative Commons licence and your intended use is not permitted by statutory regulation or exceeds the permitted use, you will need to obtain permission directly from the copyright holder. To view a copy of this licence, visit <http://creativecommons.org/licenses/by-nc-nd/4.0/>.

© The Author(s) 2025